Pérez-Esteve, É.; Oliver Hernández, L.; García López, L.; Nieuwland, M.; De Jongh, HHJ.; Martínez-Máñez, R.; Barat Baviera, JM. (2014). Incorporation of Mesoporous Silica Particles in Gelatine Gels: Effect of Particle Type and Surface Modification on Physical Properties. Langmuir. 30(23):6970-6979. doi:10.1021/la501206f.

INCORPORATION OF MESOPOROUS SILICA PARTICLES IN GELATINE GELS: EFFECT OF PARTICLE TYPE AND SURFACE MODIFICATION ON PHYSICAL PROPERTIES

Édgar Pérez-Esteve[1,2*], Laura Oliver[3,4], Laura García[1], Maaike Nieuwland[3,5], Harmen H. J. de Jongh[3,6], Ramón Martínez-Máñez[2,7], José Manuel Barat[1]

1. Grupo de Investigación e Innovación Alimentaria, Departamento de Tecnología de Alimentos, Universitat Politècnica de València, Camino de Vera s/n., 46022 Valencia, Spain
2. Centro de Reconocimiento Molecular y Desarrollo Tecnológico, Unidad Mixta Universitat Politècnica de València-Universitat de València, Camino de Vera s/n, 46022, Valencia, Spain
3. Top Institute Food & Nutrition, P.O. Box 557, 6700 AN, Wageningen, The Netherlands
4. NIZO Food Research B.V., P.O. Box 20, 6710 BA, Ede, The Netherlands
5. TNO, PO Box 360, 3700 AJ Zeist, The Netherlands
6. Wageningen University & Research Center, Food Physics Group, P.O. Box 17, 6700 AA Wageningen, The Netherlands
7. CIBER de Bioingeniería, Biomateriales y Nanomedicina (CIBER-BBN), Spain

*Corresponding author. Tel.: +34 963877365; fax: +34 963877956. E-mail address: edpees@upv.es

ABSTRACT

The aim of this work was to investigate the impact of mesoporous silica particles (MSP) on the physicochemical properties of filled protein gels. We have studied the effect of the addition of different mesoporous silica particles, either bare or functionalised with amines or carboxylates, on the physical properties of gelatine gels (5% w/v). Texture properties of the filled gels were investigated by uniaxial compression, while optical properties were investigated by turbidity. The MSP were characterised with the objective of correlate particle features with its impact on the corresponding filled gel properties. The addition of MSP (both with and without functionalization) increased the stiffness of the gelatine gels. Furthermore, functionalised MSP showed a remarkable increase in the strength of the gels and a slight reduction of the brittleness of the gels, in contrast with non-functionalised MSP which showed no effect on these two properties. Turbidity of the gels was also affected by the addition of all tested MSP, showing that the particles that formed smaller aggregates resulted in a higher contribution to turbidity. MSP are promising candidates for the development of functional food containing smart delivery systems, being also able of modulating the functionality of protein gels.

Key words: Mesoporous Silica Particles, Smart Delivery Systems, gelatine, texture properties, turbidity.

1. Introduction

Design of new functional food with nutritional and/or health declarations often requires the encapsulation, controlled release or protection of suitable bioactive agents.[1] To achieve this goal, novel smart delivery systems based on emulsions,[2] liposomes,[3] polymeric hydrogels[4] and various inorganic particles[5,6] have been reported recently.

Among them, mesoporous silica particles (MSP) have been studied as smart delivery systems in various life sciences fields such as medicine, nutrition and food technology.[7] Their unique properties e.g. an ordered and uniform pore network, an adjustable pore size (from 2.0 nm to 50 nm), a high surface area (>700 m2g-1)[8] as well as the possibility of modify their surface with organic molecules that act as bio-responsive molecular gates[9] favour the development of promising biomedical applications related to encapsulation, protection and control delivery of bioactive agents.

Different MSP have in common that their composition is based on a SiO_2-network, a mesostructure, and the presence of silanol groups on the surface. Ones differ from each other in size, shape, porous size and volume, specific surface area and density of silanol groups in the surface providing different surface charge. Despite the most studied mesoporous silica-based material is MCM-41[9,10], both as nanoparticles[11] and microparticles,[12] other MSP with different shape and porous systems e.g. SBA-15[13,14] and UVM-7[15,16] have also been employed as molecular carriers.

MSP possess most of the desired features for a smart delivery system designed to be incorporated in a food product, such as the capability to encapsulate a high amount of bioactive molecule, the possibility to control the release within the gastrointestinal tract[5, 14] or being highly stable and biocompatible.[17,18,19] However, to the best of our knowledge, there is no information in the literature about the effect of the incorporation of MSP on product appearance, texture, mouth feel, flavor, or shelf life of the final food or beverage matrixes in which they potentially could be incorporated.

One way to integrate the MSP in food systems is to incorporate them as fillers in protein gel matrixes. Mechanical properties of emulsion filled gels or composite gels for food applications have been studied.[20,21,22] These studies show that the mechanical properties of filled gels not only depend on the physico-chemical characteristics of the gel matrix or the size, shape, spatial distribution and volume fraction of the filler, but also on the strength of the interaction between the filler and the gel matrix.[23] Depending on the nature of this interaction, the fillers are, in the extremes, mechanically connected to the gel network and then increase the gel elastic modulus (“active”) or remain inert from the gel matrix and thereby weaken the gel by acting as a hindering steric contribution during gel formation (“inactive”).[24]

Bearing in mind the lack of information on studies on the interaction of silica mesoporous particles on (protein) gels, this paper evaluates the effect of the incorporation of MSP differing in particle size, shape, and bearing different surface functionalization, on the physical properties of gelatine gels, one of the most common food model systems.

2. Experimental

2.1 Chemicals

Porcine skin gelatine (type A, 300 Bloom, average molecular weight 50-100 kDa and isoelectric point pI=7.0-9.0) was purchased from Sigma. For the synthesis of the mesoporous silica particles tetraethylorthosilicate (TEOS), N-cetyltrimethylammonium bromide (CTABr), pluronic P123 (P123), triethanolamine (TEAH3), sodium hydroxide (NaOH), chloride acid (HCl), acetic acid and N-(3-trimethoxysilylpropyl)diethylenetriamine (N3) were provided by Sigma (Sigma-Aldrich Química S.L., Madrid, Spain), while N-3-(trimethoxysilyl)propyl ethylenediamine triacetic acid trisodium salt (C3) was provided by Fluorochem (Hadfield, UK).

2.2 Sample preparation

2.2.1 Mesoporous silica particles synthesis

Microparticulated MCM-41 particles (**M**) were synthesized following the so-called "atrane route",[25] according to the method described by Barat et al., 2011.[6] N-Cetyltrimethylammonium bromide (CTABr) was used as the structure-directing agent. The molar ratio of the reagents was fixed to 7 $TEAH_3$:2 TEOS:0.52 CTABr:0.5 NaOH:180 H_2O. CTABr was added to a solution of triethanolamine ($TEAH_3$) containing sodium hydroxide (NaOH) and tetraethylorthosilicate (TEOS) at 118°C. After dissolving CTABr in the solution, water was slowly added with vigorous stirring at 70°C. After a few minutes, a white suspension was formed. This mixture was aged at room temperature overnight.

Nanoparticulated MCM-41 particles (**N**) were synthesized using the procedure described by Bernardos et al., 2011.[26] The molar ratio of the reagents was fixed to: 1 TEOS:0.1 CTABr:0.27 NaOH:1000 H2O. NaOH was added to the CTABr solution, followed by adjusting the solution temperature to 95°C. TEOS was then added dropwise to the CTABr solution. The mixture was allowed to stir for 3 h yielding a white precipitate.

SBA-15 particles (**S**) were synthesized following the method reported by Zhao et al., 1988.[27] P123 was used as the structure-directing agent. The molar ratio of the reagents was fixed to: 0.017 P123:1.0 TEOS:6 HCl:196 H_2O. The preparation was performed by mixing an aqueous solution of P123 with HCl solution, and stirring for 2 h, after which the silica source, TEOS, was added. This final mixture was stirred for a further 20 h.

UVM-7 particles (**U**) were synthesised following the method presented by Comes et al., 2009,[16] based also on the "atrane route". The molar ratio of the reagents was fixed at 7 $TEAH_3$:2 TEOS:0.52 CTABr:180 H_2O. The TEOS/$TEAH_3$ mixture was heated to 120°C until no elimination of ethanol was observed. The mixture was cooled to 90°C and CTABr was added gradually in small portions, followed by dilution with water. The mixture was aged for 24h.

For all samples, after the synthesis, the resulting powder was recovered by centrifugation, washed with deionised water, and air-dried at room temperature. To prepare the final

mesoporous materials, the as-synthesized solids were calcined at 550ºC using an oxidant atmosphere for 5h in order to remove the template phase.

2.2.2 Mesoporous silica particles functionalization

The surface of the four types of particles (#) were functionalised with N-(3-trimethoxysilylpropyl) diethylenetriamine (**N3**) or with N-[3-(trimethoxysilyl)propyl]ethylenediamine triacetic acid trisodium salt (**C3**) to add positive and negative charges, respectively. To obtain **#-N3** particles, 1 g of the different MSP were suspended in 40 mL of acetonitrile and an excess of N3 (4.3 mL, 15.0 mmol/g) was then added. To obtain to obtain **#-C3** particles, 1g of the different MSP were suspended in 30 mL of water and an excess of C3 (5.5 mL, 15.0 mmol/g) was then added. Final mixtures were stirred for 5.5 h at room temperature. Finally, the solids were filtered off, washed with 30 mL of deionised water, and dried at room temperature.

2.2.3 Filled gelatine gels preparation

Gelatine gels containing 5% (w/w) of gelatine in the aqueous phases were prepared with the four types of particles (M, N, U and S) both bare (**#**) and functionalised with carboxylates **(#-C3**) and amines (**#-N3**) at different concentrations (0, 0.1, 0.25, 0.5, 0.75 and 1%, w/w).

A stock solution of gelatine in 0.2M acetate buffer (pH 5.5) (10% w/v) was prepared by allowing the gelatine to hydrate for 2 h under gentle stirring at room temperature. The gelatine was subsequently dissolved by heating at 60°C for 30 min.

MSP were dispersed, at a known volume fraction, in acetate buffer (pH 5.5) and sonicated gently to reduce particle aggregates. The required amount of the selected MSP dispersion was then mixed with the gelatine solution. For large deformation analysis, the mixture was transferred into 20 mL plastic syringes (internal diameter 20 mm) coated with a thin film of paraffin oil. For turbidity measurements, the gels were prepared into 1 cm plastic cuvettes. In both cases, the samples were left to gel and age for 22±2 h at 20°C.

2.3 Determination of particle size distribution and zeta-potential

The particle size distribution of the different bare and functionalised MSP was determined using a Malvern Mastersizer 2000 (Malvern, UK). For the measurements, samples were dispersed in acetate buffer. Data analysis was based on the Mie theory using refractive indices of 1.33 and 1.45 for the dispersant and MSP respectively. An adsorption value of 0.001 was used for all samples. Variation of this adsorption value did not significantly alter the obtained distributions. Measurements were performed in triplicate.

To determine the zeta potential (ζ) of the bare and functionalised MSP, a Zetasizer Nano ZS equipment (Malvern Instruments, UK) was used. Samples were dispersed in acetate buffer at concentration of 1 mg/mL. Before each measurement, samples were sonicated for 2 minutes to preclude aggregation. The zeta potential was calculated from the particle mobility values by applying the Smoluchowski model. The average of five recordings is reported as zeta potential. The measurement was performed at 25°C. Measurements were performed in triplicate.

2.4 Determination of functionalization degree

The functionalization degree of different particles was determined by thermogravimetric analyses. Determinations were carried out on a TGA/SDTA 851e Mettler Toledo balance, with a heating program consisting of a heating ramp of 10° per minute from 273 to 373 K followed by an isothermal heating step at this temperature for 60 min under nitrogen atmosphere (80 mL/min). Then, the program continues with a dynamic heating segment from 373 to 1273 K using an oxidant atmosphere (air, 80 mL/min) and an isothermal heating step at this temperature for 30 min.

2.5 Transmission electron microscopy (TEM)

For transmission electron microscopy (TEM) analysis MSP were dispersed in dichloromethane and sonicated for 2 minutes to preclude aggregates and the suspension was deposited onto copper grids coated with carbon film (Aname SL, Madrid, Spain). Imaging of the MSP samples was performed using a JEOL JEM-1010 (JEOL Europe SAS, France) operating at an acceleration voltage of 80 kV. The single particle size was estimated by averaging measured size values of 50 particles.

2.6 Confocal laser scanning microscopy (CLSM)

The morphologic analysis of bare and functionalised MSP particles dispersed in acetate buffer and also incorporated to gelatine were performed by confocal laser scanning microscopy after staining the samples with Rhodamine B (0.2%). CSLM images were recorded on a LEICA TCS SP Confocal Laser Scanning Microscopy (Leica Microsystems CMS GmbH., Manheim, Germany) equipped with an inverted microscope (model Leica DM IRBE), used in the single photon mode with Ar/Kr visible light laser. The excitation wavelength was set at 540 nm. Digital image files were acquired in format of 1024 x 1024 pixel resolution.

2.7 Large deformation experiments

Uniaxial compression tests were performed using a texture analyzer (TA.XT.plus Texture Analyser, Stable Micro Systems, Godalming, Surrey, United Kingdom), employing a plate probe (diameter: 75 mm). The plates were lubricated with a thin layer of paraffin oil. The gels were removed from the syringe and cut to obtain cylinders of 20 mm of diameter and 20 mm of height. The measurements were performed at a constant deformation speed of 1 mm·s^{-1} and up to a compression strain of 90%.

The relative deformation at a certain stage is expressed as a true or Hencky strain, ε_H (-), which is defined as:

$$\varepsilon_H = \int_{H_0}^{H_t} \frac{1}{H} dH = ln\left(\frac{H_t}{H_0}\right), \qquad (1)$$

where H_0 is the initial specimen height (m), and H is the actual height after certain deformation time t (m). For compression, the Hencky strain is negative, but it will be expressed as a positive figure. The average true or Hencky stress, $\sigma(t)$ (Pa), in the test piece at a certain deformation at time t is given by:

$$\sigma(t) = \frac{F(t)}{A(t)}, \qquad (2)$$

where *F(t)* is the measured force after a deformation time *t* (N), and *A(t)* is the cross-sectional area of the sample (m^2). The true stress accounts for the continuous change in the cross-sectional area assuming no change in cylindrical shape and constant volume during the compression. The apparent Young's modulus, *E* (Pa), of the sample was defined as the initial slope within the linear region of the true stress versus true strain curve. The Young's modulus is representative of the stiffness of the gel. Fracture stress and strain are defined as strength and brittleness of the gel, respectively.

2.8 Turbidity measurement

The turbidity (τ) of the gels was measured using a JASCO V-630 Spectrophotometer (JASCO Analitica Spain S.L, Madrid, Spain) at 550 nm against acetate buffer and expressed as % of transmittance. Measurements were performed in duplicate.

2.9 Statistical analysis

All tests were carried out for at least three times and data were subjected to multifactorial analysis of variance (ANOVA) using Statgraphics Centuriun XV (Manugistics Inc., Rockville, MD, USA). Results followed by the same letter in the same column are not significantly different between means ($p<0.005$).

3. Results and discussion

3.1 MSP characterization

A morphologic analysis of different synthesised MSP was performed by transmission electron microscopy (TEM). First column of figure 1 shows the evident differences in particle size, shape and also in porosity. Nanoparticulated MCM-41 particles (N) are spherical nanoparticles with an apparent pore size in the range of 2-3 nm. UVM-7 particles (U) are organized in the form of clusters of pseudo-spherical mesoporous nanoparticles. Microparticulated MCM-41 particles (M) look like porous irregular-shaped particles whose pore size is in the range of 2-3 nm. Finally, SBA-15 (S) are elongated particles with a well-defined hexagonal mesoporous distribution.

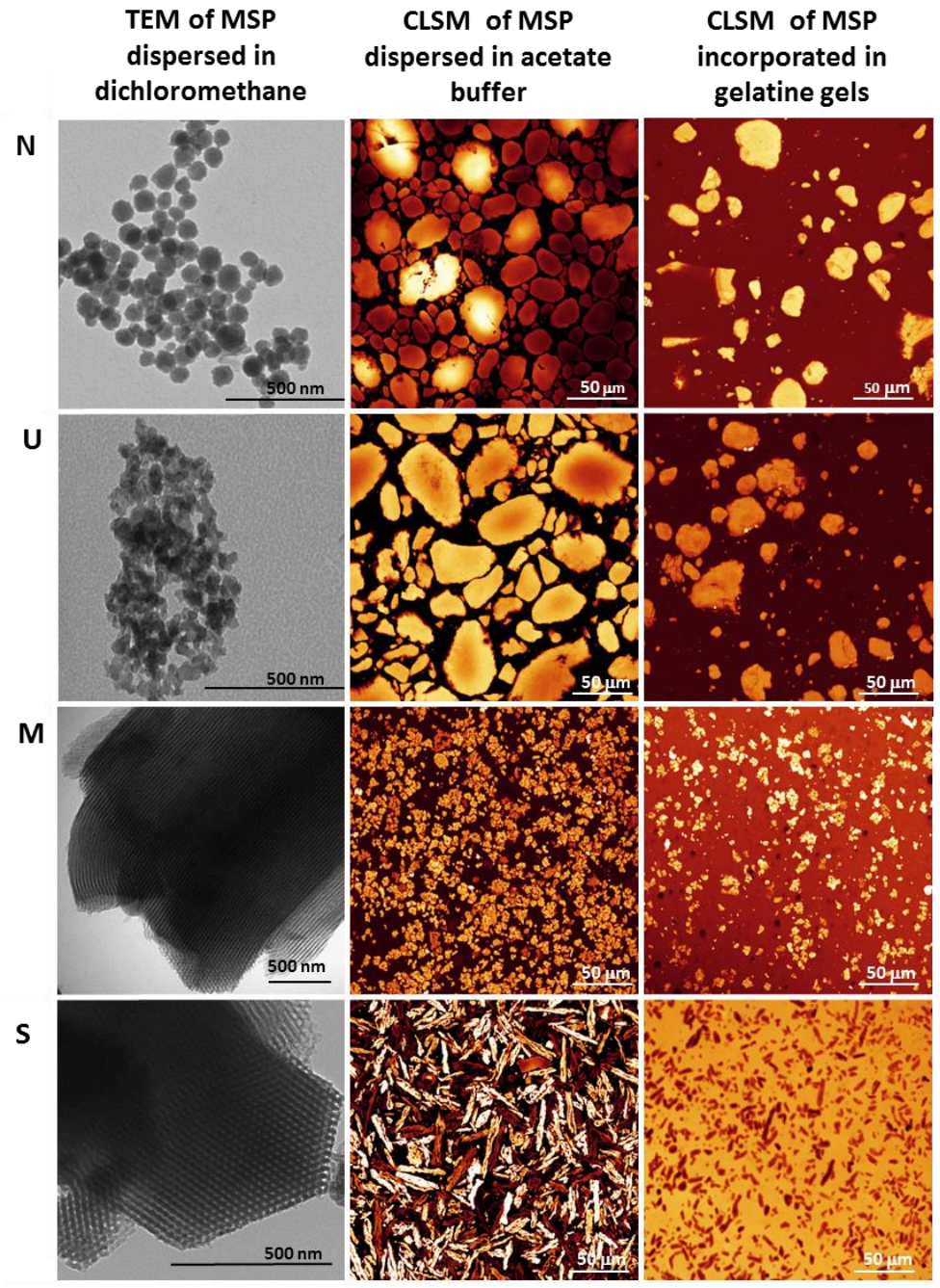

FIGURE 1. TEM (left) and CLSM images of different MSP stained with Rhodamine B dispersed in acetate buffer (middle) or incorporated in gelatine gels (right). N: Nanoparticulated MCM-41; U: UVM-7; M: Microparticulated MCM-41; S: SBA-15

Besides the shape, this morphologic analysis allowed the determination of the single particle size of different MSP. Size oscillated from ca. 100 nm of **N** to ca. 1-1.5 micron of **M** or **S**. **U** clusters had different sizes, being the average next to the micro scale. Size values are summarized in table 1.

Table 1. Size (Mean±SD) of different bare and functionalised MSP determined by TEM (dry) or Light Diffraction (dispersed in acetate buffer). N: Nanoparticulated MCM-41; U: UVM-7; M: Microparticulated MCM-41; S: SBA-15

MSP	Bare (Dry)	Bare (Acetate)	COO^- (Acetate)	NH_3^+ (Acetate)
	Single particle size (μm)	d(0.5)* (μm)	d(0.5)* (μm)	d(0.5)* (μm)
N	0.09±0.02[c]	4.79±0.04[c]	2.36±0.06[b]	0.86±0.01[b]
U	0.87±0.25[b]	6.19±0.04[b]	3.38±0.03[c]	2.62±0.08[c]
M	1.2±0.3[a]	0.82±0.01[a]	0.74±0.01[a]	0.55±0.00[a]
S	1.3±0.2[a]	0.78±0.00[a]	0.78±0.02[a]	0.63±0.01[a]

*Maximum particle diameter below which 50% of the sample exists. Values with different letters in the same column are significantly different at p-value $p<0.001$.

As the particles were incorporated into gelatine gels in a buffered aqueous dispersion, size distribution and zeta potential of the particles were also determined in acetate buffer (pH 5.5). Figure 2a shows the size distribution of the four bare particles. A direct visual inspection allows to distinguish two different groups of particles according to its size in water. On the one hand, **S** and **M**, exhibited a size distribution in the range 0.5-10 μm, while size distribution of **N** and **U** ranged from 5 up to 20μm. When single particle size obtained by TEM and size distribution obtained by the Mastersizer were compared (table 2) it was stated that particle size remained in the same range for **S** and **M**. However, size increased dramatically in the case of **N** and **U**, passing from the nanoscale to the microscale. Size of different MSP was also checked by CLSM, confirming that particle size in water suspension was in accordance with size distribution measured by Light Diffraction (figure 1 middle).

Size distribution of functionalized MSP were also determined. Figure 2b and 2c shows the size distribution of **#-C3** and **#-N3** particles respectively. For all MSP, both types of functionalization resulted in a decrease of the particle size. This difference was more significant for **N** and **U** and more pronounced in the case of functionalization with amines.

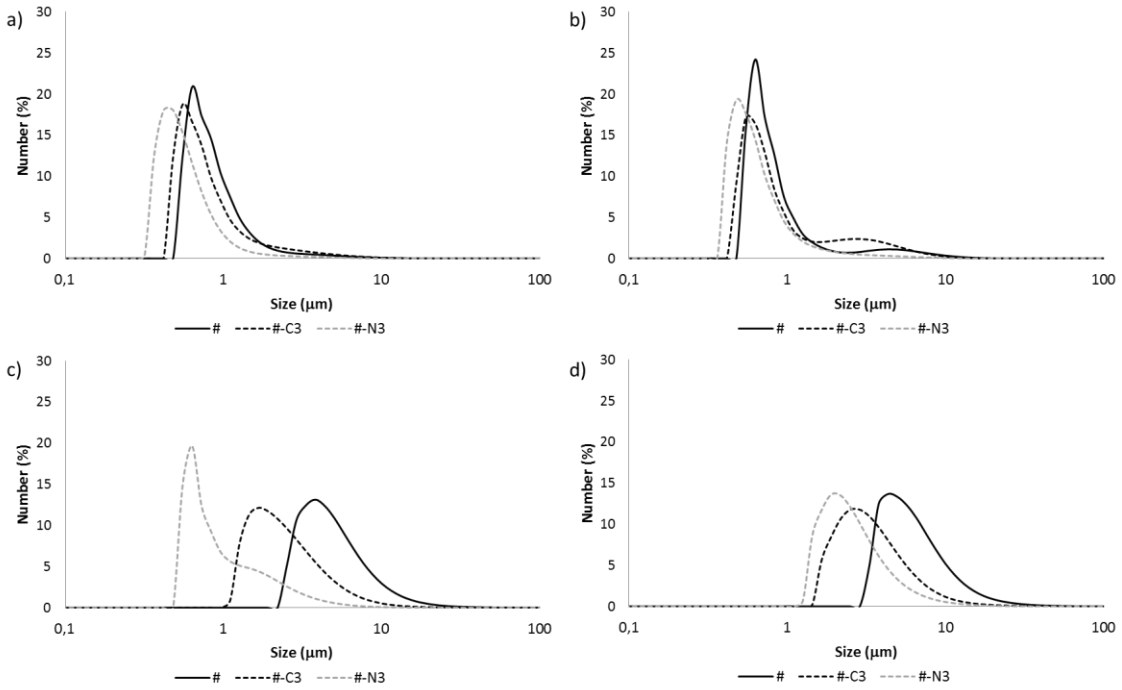

FIGURE 2. Size distribution of different MSP dispersed in acetate buffer at pH 5.5. a) Microparticulated MCM-41. b) SBA-15. c) Nanoparticulated MCM-41. d) UVM-7. #: Bare particle. #-C3: Carboxylate functionalised particle. #-N3: Amine functionalised particle.

Finally, the morphology of bare and functionalized particles after being incorporated in gelatine gels was also characterized by CLSM. The third column of figure 1 shows how the interaction of MSP with gelatine did not modify the size or shape of the particles, in comparison with the same particle in buffer dispersion (figure 1 middle).

3.2 Functionalization characterization

The functionalization degree solids **#-C3** and **#-N3** was determined by thermogravimetric analyses (see Table 2). As it can be seen, a similar functionalization was observed for the different materials when functionalised with **N3** or **C3**. However for a given material if the **C3** and **N3** functionalization are compared, it is apparent from the data that the amount **N3** anchored to the particles (ca. 40 mg g^{-1} SiO_2) is higher than the amount of **C3** (ca. 30 mg g^{-1} SiO_2). This was somehow expected and can be explained taking into account that **C3** is a bulkier molecule than **N3**.

Table 2. Content of organic molecules anchored to the particles after functionalization.

MSP	Carboxylate functionalised (mg C3 g^{-1} SiO_2)	Amine functionalised (mg N3 g^{-1} SiO_2)
N	32.2	40.3
U	34.7	44.2
M	35.4	43.2
S	33.2	42.5

The efficiency of functionalization was also tested by zeta potential determinations. Figure 3 shows the zeta potential values of different MSP suspended in acetate buffer. For bare particles, two groups could be distinguished. On the one hand, **S** and **M** particles exhibited a zeta potential near to -30mV. On the other hand, **U** and **N** showed zeta potential values next to -10 mV. After functionalization with carboxylates, zeta potential values became more negative for all types of particles. In contrast, zeta potential changed from negatively to positively values after functionalization with amines, confirming the effect of the functionalization on the surface charge. For both kind of functionalization, zeta potential achieved values of -30 or +30 mV.

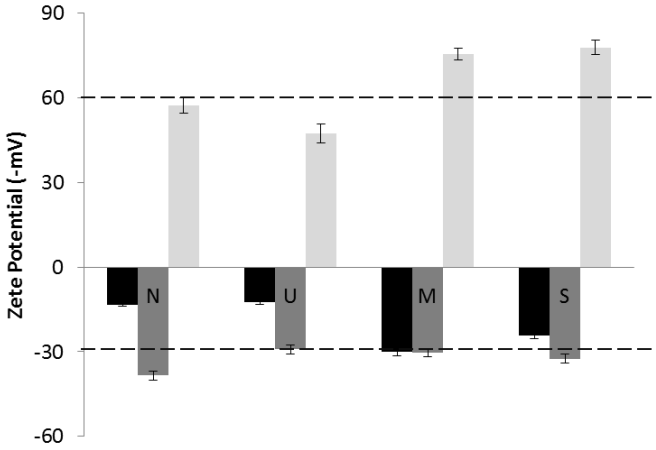

FIGURE 3. Zeta potential values (Mean±SD) of different bare (black), carboxylate functionalised (dark grey) and amine functionalised (light grey) MSP dispersed in acetate buffer (pH 5.5). N: Nanoparticulated MCM-41; U: UVM-7; M: Microparticulated MCM-41; S: SBA-15.

Zeta potential measurements also explain the changes or preservation of particle size after functionalization. The general dividing line between stable and unstable suspensions is taken at either +30 or −30 mV. Particles with zeta potentials more positive than +30 mV or more negative than −30 mV are normally considered stable.[28] This fact explain why bare **N** and **U** (particles that exhibited a zeta potential of ca. -10 mV) increased dramatically its size from the nanoscale to the microscale in aqueous suspension as a consequence of particle aggregation,

while particle distribution of **S** and **M** (zeta potential value of ca. -30 mv) remained in the same order. Values of zeta potential also allowed explaining why **N** and **U** decreased its size after functionalization with amines or carboxylates, due to the stability improvement.

3.2 Effect of MSP on large deformation properties of the gelatine gel matrix

The effect of the incorporation of different MSP on the texture properties of gelatine gels was studied by comparison of modulus and fracture properties of gelatine gels containing different percentages of MSP with those gels without particles.

3.2.1 Effect on the Young's Modulus

Figure 4 shows the Young´s modulus of gels containing different concentration of bare and functionalised MSP. The addition of the 4 types of bare MSP (Figure 4a) did not modify significantly ($p>0.5$) the Young's modulus at the concentrations studied. Although silicate species have shown to interact through both electrostatic and hydrogen bonding interactions with some poly-aminoacids and proteins,[29] the interactions with the polymeric matrix are ineffective under acidic pH.[30] Thus, due to the gels under investigation were prepared at pH 5.5, interactions between bare MSP and gelatine are expected to be very week.

The same behaviour was found for **#-C3** particles (Fig. 4b). However, when **M-N3**, **N-N3**, and **S-N3** were incorporated in the gel matrix a significant increase of Young's modulus ($p<0.05$) was observed. The Young's modulus of gels filled with U-N3 did not increase significantly.

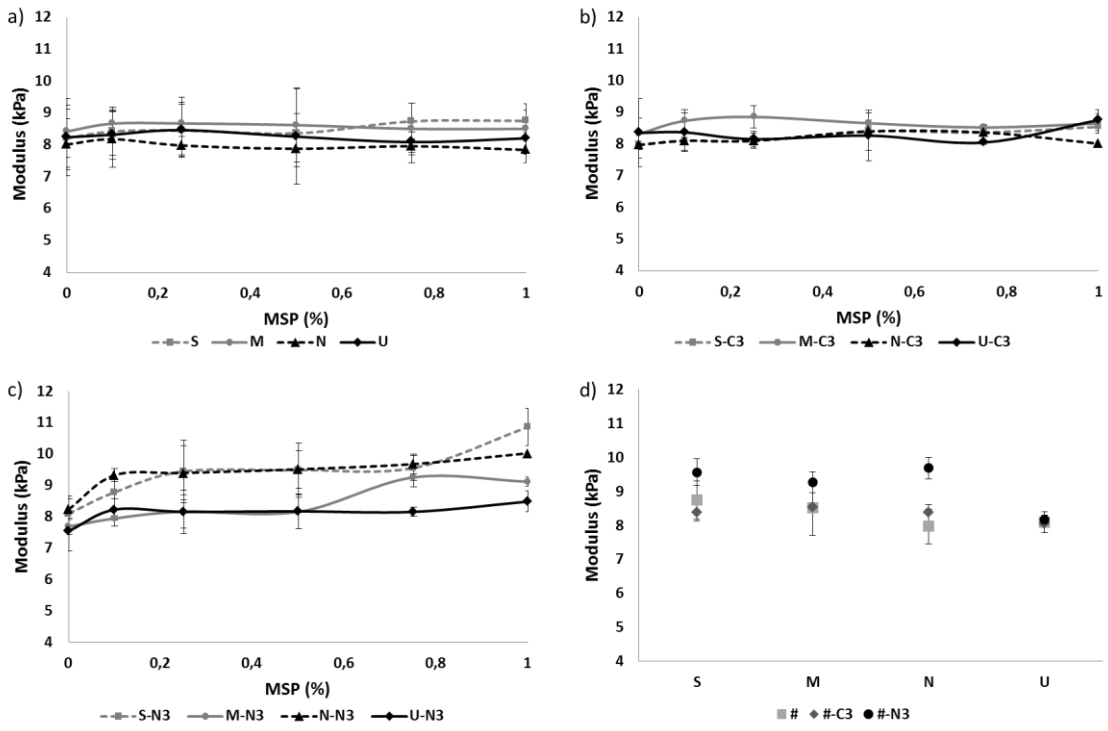

FIGURE 4. Effect of MSP concentration on the Young's Modulus of gelatine gels. a) Bare MSP, b) MSP functionalised with carboxylates. c) MSP functionalised with amines, d) Comparison of values of Young's Modulus at the concentration of 0.75%. N: Nanoparticulated MCM-41; U: UVM-7; M: Microparticulated MCM-41; S: SBA-15. #: Bare particle. #-C3: Carboxylate functionalised particle. #-N3: Amine functionalised particle.

To be able to compare the effect of the kind of particle on the stiffness of the gels, values of Young's Modulus of gels containing 0.75% of particles are plotted in figure 4d. The figure shows no significant differences between gels filled with **#** and **#-C3** particles. However, when gels were filled **#-N3** particles, the effect of particle type was significant for **M**, **N** and **S** type particles.

From these results, it could be concluded that the presence of MSP type and functionalization does not affect the stiffness of the gels by themselves. However, when functionalization is able to decrease the size of a particle cluster, particle type and amine or carboxylate functionalization become relevant for final gel stiffness.

This is in agreement with Fu et al., 2008,[31] who described that there are three decisive factors determining the elastic modulus of a filled-polymer gel: the elastic modulus of the filler and the matrix (the higher the elastic modulus of the filler, the higher the elastic modulus of the composite), the filler concentration and the aspect ratio of the filler. Next to that, the interaction of the filler with the matrix is an important factor, determining if the filler is active or inactive,[24]. In this particular case, the Young's modulus of SiO_2, is much higher than that of gelatine, however the concentration of particles was not enough to raise the Young´s modulus. The most important factors were the size of the filler and the aspect ratio, justifying why M, N and S had different contributions to the increase of the Young's modulus.

In neither case the gel strength was negatively affected by the presence of the particles, indicating that the particles act as active filler. Especially for the **#-N3** particles, the interaction between particles and gel matrix is expected to be strong.

3.2.2 Effect on fracture stress

The effect of MSP content on fracture stress is shown in figure 5. Bare MSP (Figure 5a) did not modify values of fracture stress, and thus, did not affect gel strength. However, when particles were functionalized with carboxylates or with amines (Figure 5b and c), particles contributed to the increase of final gel strength proportionally with concentration. In spite of the functionalization, **U** was the particle that contributed to the gel strength in a less pronounced manner. In contrast, **N** contributed the most to fracture stress values. Bearing in mind that **U** formed large aggregates that did not modify significantly their size as a consequence of the functionalization and that **N** aggregates decreased noticeably the size after functionalization, the importance of particle size on fracture stress values is confirmed. Figure 5 also displays the

dependence of particle concentration on gel strength, since for each particle a minimum concentration is needed to vary significantly the value of fracture stress.

According to these results, it could be stated that the combination of particle size, particle concentration and organic functionalization are the three parameters that affect the strength of the filled gels.

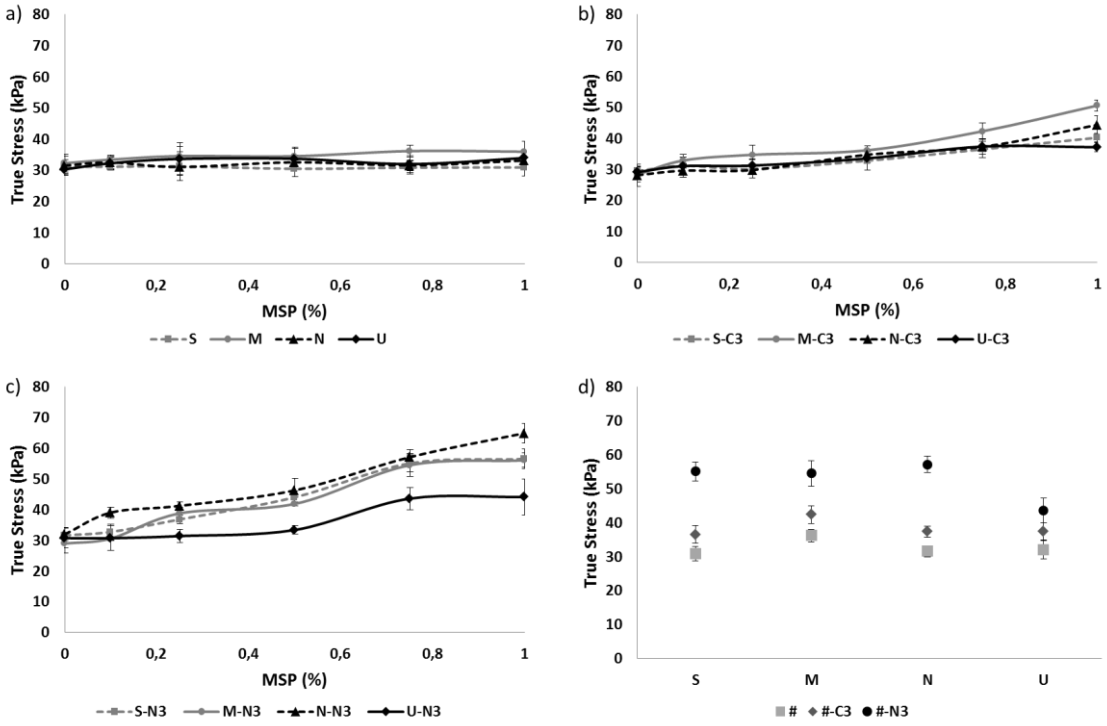

FIGURE 5. Effect of MSP concentration on the Fracture Stress of gelatine gels. a) Bare MSP, b) MSP functionalised with carboxylates. c) MSP functionalised with amines, d) Comparison of values of Young's Modulus at the concentration of 0.75%. N: Nanoparticulated MCM-41; U: UVM-7; M: Microparticulated MCM-41; S: SBA-15. #: Bare particle. #-C3: Carboxylate functionalised particle. #-N3: Amine functionalised particle.

3.2.3 Effect on fracture strain

Figure 6 shows the effect of MSP concentration on fracture strain of gelatine gels. As occurred for Young's modulus and fracture stain, the addition of different concentration of the four types of bare MSP did not provoke significant changes in fracture strain values. Instead, gels filled with functionalised MSP exhibited a significant increase ($p<0.005$) on the fracture strain in comparison with the control gel. The presentation of values of fracture strain for gels filled with different bare and functionalized particles in the same graph (fig. 6d) confirmed that the

highest fracture strain values are apparent in gels filled with particles functionalized with amines, followed by gels filled with particles functionalized with carboxylates. Accordingly, it could be concluded that the functionalization is more important than the particle size or shape for fracture stress.

This improvement of the strain at fracture of a polymer-network by the incorporation of hybrid nanofillers (inorganic nanoparticles with organic surface) has been also reported by other authors[32] and is related to a better filler-matrix interaction, increasing the integrity and stability of the gel and thus making it withstand more deformation before energy dissipates via (micro-) fracture-events.

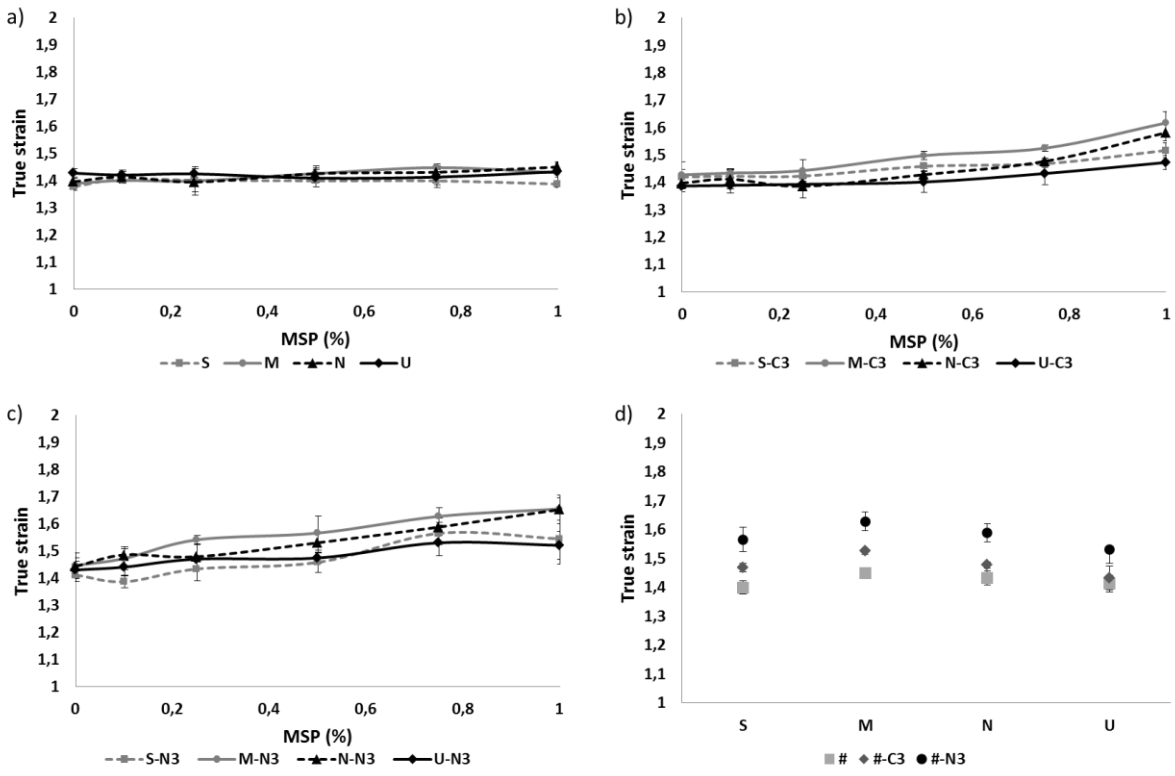

FIGURE 6. Effect of MSP concentration on Fracture Strain of gelatine gels. a) Bare MSP, b) MSP functionalised with carboxylates. c) MSP functionalised with amines, d) Comparison of values of Young's Modulus at the concentration of 0.75%. N: Nanoparticulated MCM-41; U: UVM-7; M: Microparticulated MCM-41; S: SBA-15. #: Bare particle. #-C3: Carboxylate functionalised particle. #-N3: Amine functionalised particle.

3.2.4 Effect of particle size and surface modification on the filler-matrix interaction

Two ideas are clear after evaluating the effect of the addition of **#**, **#-C3** and **#-N3** particles at concentrations from 0-1% on textural properties of gelatine gels. On one hand, organic functionalization is needed to improve the Young's modulus and fracture properties while on the other hand, a minimum concentration of particle (different for each kind or particle) should be achieved to observe this phenomenon.

Figure 7 tries to explain graphically the influence of particle size, shape and surface modification on filler-matrix interaction. Bare particles that are next to the instable zone tend to aggregate. Moreover, at acidic pH, interactions between bare MSP and gelatine are expected to be very week (figure 7a). After carboxylate and amine functionalization, particles add organic molecules to their surface and achieve a zeta potential able to stabilize the particle, reducing the aggregation tendency. These organic molecules also improve the compatibility between the particle and the protein matrix and generate an interfacial area in the surroundings of the particles (figure 7b). The interfacial area consists of immobilized proteins whose structure and properties change because of the interaction with the particles. [32,33]

Large particles or low concentration will result in a low absolute number or particles embedded in the matrix. Low number of particles implies that the relative distance between them is too large and the interfacial area of each particle remains isolated from the rest (figure 6b). For small sized particles or high volume fractions, the interfacial areas of each particle start to overlap (figure 7c), resulting in an intensification of the interactions[34] and reinforcing the protein network and thus increasing both the Young's Modulus and fracture properties.

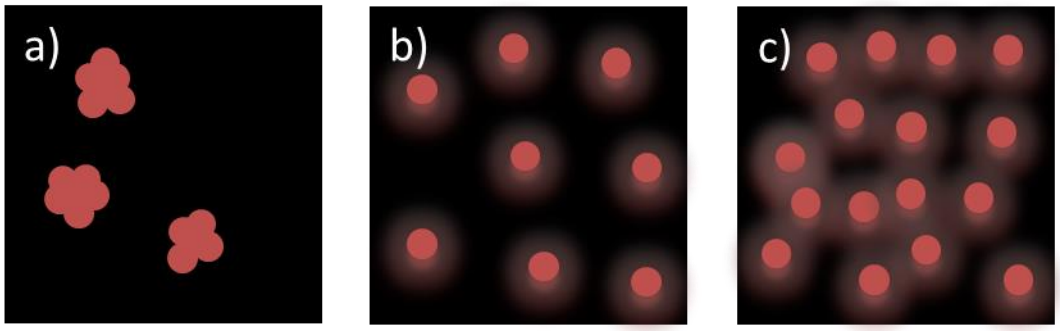

FIGURE 7. a) Scheme of the structure of a filled gel: bare MSP (red spheres). b) Interfacial area formation (diffuse layer in particle surroundings) under low concentration of functionalised particles (large distance between interfacial areas). c) Interfacial area formation under high concentration of functionalised particles (overlap of interfacial areas, increase of bounding between layers).

3.3 Effect of MSP on gel turbidity of the gelatine gel matrix

The effect of bare and functionalised MSP at different concentration on turbidity of filled-gelatine gels expressed as percentage of transmittance is shown in figure 8. Non-filled gels exhibited values of transmittance of 92±2%. The subsequent addition of bare or functionalised MSP decreased the transmittance of the sample as a function of particle concentration, thereby increasing the turbidity of the gel. At low concentrations (0.1 and 0.25%) figure 8 allows to evaluate most explicit the different contribution of each of the particle to the final turbidity. This is consistent with light scattering theory, which states that for moderately dilute suspensions of particles, there is an exponential decrease in transmitted light with particle concentration.[35] However, from concentrations up to 0.5% of particles, turbidity dramatically increases achieving the transmittance values next to 0.

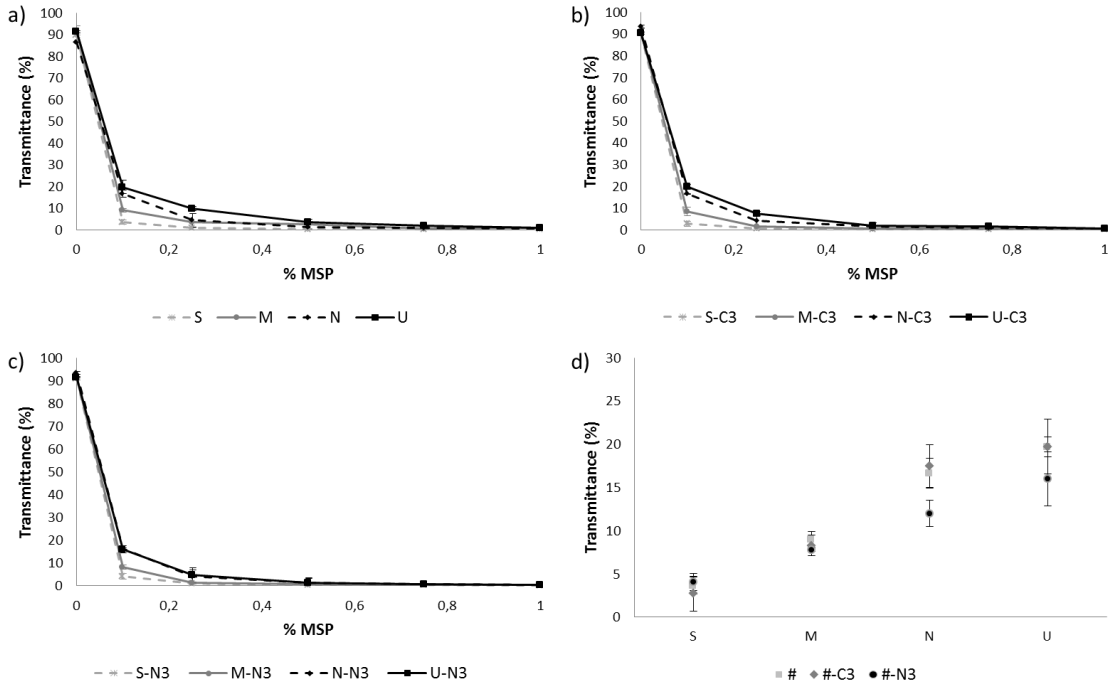

FIGURE 8. Effect of MSP concentration on gel turbidity expressed as % of transmittance. a) Bare MSP, b) MSP functionalised with carboxilates. c) MSP functionalised with amines, d) Comparison of transmittance at the concentration of 0.1%. N: Nanoparticulated MCM-41; U: UVM-7; M: Microparticulated MCM-41; S: SBA-15. #: Bare particle; #-C3: Caroxylate functionalised particle; #-N3: Amine functionalised particle

To understand the effect of particle size, shape and functionalization on gel turbidity, values of turbidity of gels filled with 0.1% of particle has been plotted separately in figure 8.d. This figure shows that gel turbidity is related with the particle size determined with the Mastersizer, so that contribution of small particles to final turbidity is higher than large particles. Higher absolute number of particles provokes a larger decrease of transmitted light. Since the gelatine gels are prepared based on mass concentration of the MSP, for the same mass concentration there are more small particles and transmitted light decreases more drastically.

This effect is corroborated by the fact that particles that did not alter their size significantly as a function of functionalization (**S** and **M**) maintained turbidity values independent of the functionalization. Gels filled with particles that changed their size by functionalization (**N** and **U**) exhibit a different turbidity when the particles were functionalized with amines and thereby reduced its size significantly.

Thus, the incorporation of MSP in gelatine gels affects the gel turbidity as a function of particle size and concentration, providing opacity of the gels at concentrations up to 0.5% of MSP present. To obtain transparent filled gels a lower particle concentrations would be needed.

4. Conclusions

In this study four different MSP has been successfully functionalised, characterized and incorporated in gelatine gels. The characterization process stated that particles experience a significant change in the aggregation tendency after carboxylate or amine functionalization, therefore modifying their particle/clusters size. Particle functionalization also creates an organic layer on the surface of the particle that improves the filler-matrix interaction. This causes an increase of the Young's modulus, fracture stress and fracture strain, more or less pronounced depending on the kind of particle, functionalization and concentration. Gelatine gels filled with bare particles at concentrations between 0-1% maintain their textural properties. The most affected property is turbidity, which increases with the addition of both bare and functionalised MSP. These findings lead us to conclude that the mechanical properties of the filled gels remain or improve with the addition of MSP and that although not being suitable for transparent systems, MSP are promising delivery systems able to be incorporated in food like products.

Acknowledgements

Authors gratefully acknowledge the financial support from the Ministerio de Economía y Competitividad (Projects AGL2012-39597-C02-01, AGL2012-39597-C02-02 and MAT2012-38429-C04-01) and the Generalitat Valenciana (project PROMETEO/2009/016). E.P. is grateful to the Ministerio de Ciencia e Innovación for his grant (AP2008-00620). Saskia de Jong (NIZO food research) is acknowledged for assistance during CLSM observations and rheology interpretation.

REFERENCES

(1) Weiss, J.; Takhistov, P; McClements, J. Functional materials in food nanotechnology. *J. Food Sci.* **2006**, 71(9), R107-R116.

(2) Anton, N.; Mojzisova, H.; Porcher, E.; Benoit, J.P.; Saulnier, P. Reverse micelle-loaded lipid nano-emulsions: new technology for nano-encapsulation of hydrophilic materials. *Int. J. Pharm.* **2010**, 398, 204-209.

(3) An, X.; Zhan, F.; Zhu, Y. Smart photothermal-triggered bilayer phase transition in AuNPs–liposomes to release drug. *Langmuir* **2013**, 29, 1061–1068.

(4) Chaturvedi, K.; Ganguly, K.; Nadagouda, M.N.; Aminabhavi, T.M. Polymeric hydrogels for oral insulin delivery. *J. Control. Release* **2013**, 165, 129-138.

(5) Bernardos, A.; Aznar, E.; Coll, C.; Martínez-Máñez, R.; Barat, JM.; Marcos, M.D.; Sancenón, F.; Benito, A.; Soto, J. Controlled release of vitamin B2 using mesoporous materials functionalized with amine-bearing gate-like scaffoldings. *J. Control. Release* **2008,** 131, 181-189

(6) Barat, J. M.; Pérez-Esteve, E.; Bernardos, A; Martínez-Máñez, R. Nutritional effects of folic acid controlled release from mesoporous materials. *Procedia Food Sci*. **2011**, 1, 1828-1832.

(7) Pérez-Esteve, E.; Bernardos. A.; Martínez-Máñez, R.; Barat, J. M. Nanotechnology in the development of Novel Functional Foods or their Package. An Overview Based in Patent Analysis. *Recent Pat. Food Nutr. Agric.* **2013**, 4, 172-178.

8) Vallet-Regí, M.; Balas, F; Arcos, D. Mesoporous Materials for Drug Delivery. *Angew. Chem*. *Int.* **2007**, 46, 7548-7558.

(9) Aznar, E.; Martínez-Máñez, R.; Sancenón, F. Controlled release using mesoporous materials containing gate-like scaffoldings. *Expert Opin. Drug Deliv.* **2009**, 6, 643-655.

(10) Zhao, X. S.; Lu, G. Q.; Millar, G. J. Advances in mesoporous molecular sieve MCM-41. *Ind. Eng. Chem. Res.,* **1996**, 35, 2075-2090.

(11) Salonen, J.; Laitinen, L.; Kaukonen, A.M.; Tuura, J.; Björkqvist, M.; Heikkilä, T.; Vähä-Heikkilä, K.; Hirvonen, J.; Lehto, V.P. Mesoporous silicon microparticles for oral drug delivery: loading and release of five model drugs. *J Control Release* **2005**, 108, 362-374

(12) Trewyn, B. G.; Slowing, I. I.; Giri, S.; Chen, H. T.; Lin, V. S. Synthesis and functionalization of a mesoporous silica nanoparticle based on the sol-gel process and applications in controlled release. *Acc Chem Res.* **2007,** 40, 846-853.

(13) Rahmat, N.; Abdullah, A.Z.; Mohamed, A.R. A review: mesoporous Santa Barbara amorphous-15, types, synthesis and its applications towards biorefinery production. Am. J. Appl. Sci. ***2010***, 7, 1579–1586

(14) Song, S.-W.; Hidajat, K.; Kawi, S. Functionalized SBA-15 materials as carriers for controlled drug delivery: influence of surface properties on matrix−drug Interactions. *Langmuir*, **2005**, 21 9568–9575

(15) Jamal El Haskouri,a David Ortiz de Zárate,a Carmen Guillem,a Julio Latorre,a Maite Caldés,b Aurelio Beltrán,a Daniel Beltrán,a Ana B. Descalzo,c Gertrudis Rodríguez-López,c Ramón Martínez-Máñez,c M. Dolores Marcos*c and Pedro Amorós*a Silica-based powders and monoliths with bimodal pore systems. Chem. Commun., 2002, 330-331

(16) Comes, M.; Aznar, E.; Moragues, M.; Marcos, M. D.; Martínez-Máñez, R.; Sancenón, F.; Soto, J.; Villaescusa, L. A.; Gil, L; Amorós, P. Mesoporous hybrid materials containing nanoscopic "binding pockets" for colorimetric anion signaling in water by using displacement assays. *Chem. Eur. J.* **2009**, 15, 9024-9033.(17) Moon, D.-S.; Lee, J.-K. Tunable Synthesis of Hierarchical Mesoporous Silica Nanoparticles with Radial Wrinkle Structure. *Langmuir* **2012**, 28, 12341–12347.

(18) Asefa, T.; Tao, Z. Biocompatibility of Mesoporous Silica Nanoparticles. *Chem. Res. Toxicol*. **2012**, 25, 2265–2284.

(19) Mamaeva, V.; Sahlgren, C.; Lindén, M. Mesoporous silica nanoparticles in medicine—Recent advances. *Adv Drug Deliv Rev.* **2013**, 65, 689-702.

(20) Sala, G.; Van Vliet, T.; Cohen Stuart, M. A.; Van Aken, G. A.; Van de Velde, F. Deformation and fracture of emulsion-filled gels. Effect of gelling agent concentration and oil droplet size. *Food Hydrocolloids* **2009**, 23, 1853-1863.

(21) Sala, G. ,Van Vliet, T., Cohen Stuart, M.A., Van Aken, G.A., Van de Velde, F., Deformation and fracture of emulsion-filled gels. Effect of oil content and deformation speed. *Food Hydrocoloids* **2009**; 23, 1381-1393.

(22) Lorenzo, G.; Zaritzky, N.; Califano, A. Rheological analysis of emulsion-filled gels based on high acyl gellan gum. *Food Hydrocolloids* **2013**, 30, 672-680.

(23) van Vliet, T. Rheological properties of filled gels. Influence of filler matrix interaction. *Colloid. Polym. Sci.* **1988**, 266, 518-524.

(24) Ring, S.; Stainsby, G. Filler reinforcement of gels. *Prog. Food Nutr. Sci.* **1982**, 6, 355-361.

(25) Cabrera, S.; Haskouri, J.E.; Guillem, C.; Latorre, J.; Beltrán-Porter, A.; Beltrán-Porter, D.; Marcos, M.D.; Amorós, P. Generalised syntheses of ordered mesoporous oxides: the atrane route. *Solid State Sci.* **2000**, 4, 405–420

(26) Bernardos, A.; Mondragón, L.; Aznar, E.; Marcos, M.D.; Martínez-Máñez, R.; Sancenón, F.; Soto, J.; Barat, J.M.; Pérez-Payá, E.; Guillem, C. & Amorós, P. Enzyme-responsive intracellular controlled release using nanometric silica mesoporous supports capped with 'saccharides'. *ACS nano* **2011**, 4, 6353-6368.

(27) Zhao, D.; Huo, Q.; Feng, J.; Chmelka, B.F.; Stucky, G.D. Nonionic triblock and star diblock copolymer and oligomeric surfactant syntheses of highly ordered, hydrothermally stable, mesoporous silica structures. *J. Am. Chem. Soc.* **1998**, 120, 6024-6036.

(28) Duman, O., Tunç, S. Electrokinetic and rheological properties of Na-bentonite in some electrolyte solutions. *Micropor. Mesopor. Mater*. **2009**, 117, 331–338.

(29) Fernandes, F.; Manjubala, I.; Ruiz-Hitzky, E. Gelatin renaturation and the interfacial role of fillers in bionanocomposites. *Phys. Chem. Chem. Phys.* **2011**, 13, 4901–4910.

(30) Coradin, T.; Bah, S; Livage, J. Gelatine/silicate interactions: from nanoparticles to composite gels. *Colloids Surf., B* **2004**, 35; 53-58.

(31) Fu, S.; Feng, X; Lauke, B.; Mai, J. Effects of particle size, particle/matrix interface adhesion and particle loading on mechanical properties of particulate–polymer composites. *Composites Part B* **2008**, 39, 933–961.

(32) Tjong, S. Structural and mechanical properties of polymer nanocomposites. *Mat. Sci. Eng. R.* **2006**, 53: 73–197.

(33) Pitsa, D.; Danikas, M. Interfaces features in polymer nanocomposites: A review of proposed models. *Nano* **2011**, 6, 497-508.

(34) Vaia, R.; Wagner, D. Framework for nanocomposites. *Mater. Today* **2004**, 7, 32-37.

(35) Gregory, J. Turbidity and Beyond. *Filtr. Separat.* **1998**, 35, 63-67.

GRAFICAL ABSTRACT